Dalton Transactions

Electrochemical properties and C-H bond oxidation activity of $[Ru(tpy)(pyalk)Cl]^+$ and $[Ru(tpy)(pyalk)(OH)]^+$

Journal:	*Dalton Transactions*
Manuscript ID	DT-ART-06-2018-002260.R1
Article Type:	Paper
Date Submitted by the Author:	23-Jun-2018
Complete List of Authors:	Nilles, Christian; North Dakota State University, Department of Chemistry and Biochemistry Herath, Hashini; North Dakota State University, Department of Chemistry and Biochemistry Fanous, Hanna; North Dakota State University, Department of Chemistry and Biochemistry Ugrinov, Angel; North Dakota State Univeristy, Dept of Chemistry and Biochemistry Parent, Alexander; North Dakota State University, Department of Chemistry and Biochemistry

SCHOLARONE™
Manuscripts

Please do not adjust margins

Journal Name

ARTICLE

Electrochemical properties and C-H bond oxidation activity of $[Ru(tpy)(pyalk)Cl]^+$ and $[Ru(tpy)(pyalk)(OH)]^+$

0Received 00th January 20xx,
Accepted 00th January 20xx

DOI: 10.1039/x0xx00000x

www.rsc.org/

C. K. Nilles,[a] H. Herath,[a] H. Fanous,[a] A. Ugrinov[a] and A. R. Parent[a]

[Ru(tpy)(pyalk)Cl]Cl (pyalk = 2-(2'-Pyridyl)-2-propanol) was synthesized and characterized crystallographically and electrochemically. Upon dissolution in water and acetonitrile, [Ru(tpy)(pyalk)Cl]Cl was found to form $[Ru(tpy)(pyalk)Cl]^+$ and $[Ru(tpy)(pyalk)(OH)]^+$, respectively. The Ru(II/III) couple of $[Ru(tpy)(pyalk)Cl]^+$ was found to be relatively low compared to that of other Ru complexes in acetonitrile, but the Ru(III/IV) couple was not significantly different than other Ru complexes bearing anionic ligands. Pourbaix diagrams were generated for $[Ru(tpy)(phpy)(OH_2)]^+$ (phpy = 2-phenylpyridine) and $[Ru(tpy)(pyalk)(OH)]^+$ in water, and it was found that $[Ru(tpy)(pyalk)(OH)]^+$ has a lower Ru(II/III) potential than $[Ru(tpy)(phpy)(OH_2)]^+$ under neutral to alkaline pH. $[Ru(tpy)(pyalk)(OH)]^+$ was found to catalyze C-H bond hydroxylation of secondary alkanes and epoxidation of alkenes using cerium(IV) ammonium nitrate as the primary oxidant.

Introduction

C-H bond activation reactions are one of organic chemistry's most fundamental tools.[1–3] These reactions typically employ a transition metal catalyst to reduce the kinetic barrier for breaking the C-H bond. Due to their importance, a significant amount of effort has been spent increasing the selectivity,[4,5] expanding the substrate scope,[6–8] and improving the sustainability of these C-H bond activation catalysts.[9–12] One key area of C-H bond activation is oxidation of the C-H bonds to form C-OH or C=O bonds.[5,12] Typically, this C-H bond oxidation proceeds via the formation of a high-valent metal oxo or oxyl species generated by reaction of a transition metal catalyst with a sacrificial chemical oxidant. This high-valent oxo species can then participate in two-electron insertion into the C-H bond, or H-atom abstraction followed by radical rebound (Scheme 1).[8] The selectivity and substrate scope of the C-H bond oxidation reaction is determined by the pathway followed, which in turn is dependent on the nature of the high-valent oxo species.[13,14]

Among the best characterized C-H bond oxidation catalysts are those based on Ru.[4,15–17] In particular, the redox properties of Ru-based coordination catalysts have been characterized for a wide variety of ligand scaffolds. Despite their well-established redox chemistry,[18–25] relatively few Ru complexes containing inner-sphere anionic ligands have been reported as C-H bond oxidation catalysts. In particular, the authors are aware of only one prior example of a Ru alkoxide complex being used to catalyze C-H bond oxidation.[25]

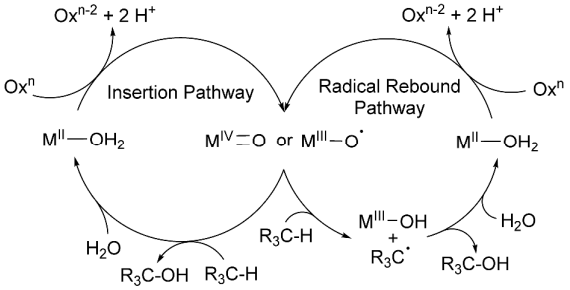

Scheme 1. General catalytic cycle for transition metal catalyzed C-H bond hydroxylation. Ox = two-electron sacrificial oxidant, M = transition metal.

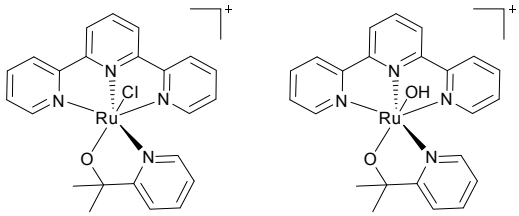

$[Ru(tpy)(pyalk)Cl]^+$ **1** $[Ru(tpy)(pyalk)OH]^+$ **2**

Chart 1. Structures of Ru coordination complexes studied in this manuscript.

Our group is interested in developing new C-H bond activation catalysts with lower redox potentials, thereby enabling the use of more sustainable oxidants in these reactions. We hypothesized that anionic ligands can be used to achieve C-H bond oxidation catalysis at these lower potentials. In order to test this hypothesis, we have synthesized $[Ru(tpy)(pyalk)Cl]^+$, **1**, and $[Ru(tpy)(pyalk)(OH)]^+$, **2**, (Chart 1), Ru complexes with a strong-donor alkoxide ligand, and characterized their redox properties and ability to catalyze C-H bond oxidation.

[a] *Department of Chemistry and Biochemistry, North Dakota State University, PO Box 6050, Fargo ND 58108-6050*

Electronic Supplementary Information (ESI) available: MS of **1**, additional electrochemical and C-H bond oxidation results. See DOI: 10.1039/x0xx00000x

Please do not adjust margins

Experimental Methods

General

2,2':6',2''-Terpyridine and cyclooctane were purchased from Alfa Aesar and used without further purification. 2-phenylpyridine, acetophenone, and N-ethylmorpholine were purchased from VWR and used without further purification. Ethylbenzene was purchase from Thermo Fisher Scientific and used without further purification. Anhydrous magnesium sulfate was purchased from AMRESCO, Inc. and used without further purification. Deuterated solvents, methylmagnesium iodide, 2-acetylpyridine, ruthenium(III) chloride hydrate, 3-(trimethylsilyl)propionic-2,2,3,3-d_4 acid sodium salt, potassium chloride, sodium periodate, hydrogen peroxide, cyclooctene oxide, cis-cyclooctene, cyclooctanone, silver chloride, ferrocene, sodium tetraphenylborate and Celite® 545 were purchased from Sigma-Aldrich Co. and were not further purified. Ammonium cerium(IV) nitrate was purchased from Strem Chemicals Inc. and used without further purification. Column chromatography was performed using RediSep® GOLD columns on a CombiFlash RF+ from Teledyne Instruments, Inc.

Synthesis of 2-(2'-Pyridyl)-2-propanol (pyalkH)

2-(2'-Pyridyl)-2-propanol was synthesized according to the published procedure.[26] In brief, 14.5 mL of 3.0 M methylmagnesium iodide (43.5 mmol, 1.2 equivalents) was added dropwise to a solution of 2-acetylpyridine (4 mL, 1.08 g/mL, 35.7 mmol) in diethyl ether (30 mL) in an ice bath. The solution was removed from the ice bath and allowed to warm to room temperature while being stirred for 2 hours. The reaction was then quenched with 30 mL of water and acidified with concentrated hydrochloric acid until both phases were clear. The aqueous layer was separated and extracted with diethyl ether (3 x 50 mL). The organic fractions were dried with magnesium sulfate, and purified using column chromatography (3:1 ethyl acetate:hexanes). The product was isolated as a hygroscopic, clear, light yellow oil.

Synthesis of [Ru(tpy)Cl_3]

[Ru(tpy)Cl_3] was synthesized according to the literature procedure.[27] In brief, 529 mg (2.35 mmol) of $RuCl_3 \cdot nH_2O$ and 465 mg (1.99 mmol) of tpy was added to 250 mL of ethanol and refluxed for 3 hours. The solution was then cooled to RT, filtered, and washed with cold EtOH and Et_2O to yield 527.4 mg (63.0%) of product after drying.

Synthesis of [Ru(tpy)(phpy)Cl] (3)

[Ru(tpy)(phpy)Cl] was synthesized according to the literature procedure.[28] In brief, 173 mg (380 µmol) of [Ru(tpy)Cl_3] and 70 µL (490 µmol) of phpy were added to 18 mL of a 1:5 H_2O:MeOH solution. N-ethylmorpholine (8 drops) was added to the solution, and it was refluxed under N_2 for 4 hours. The solution was then cooled to RT, filtered, and the precipitate was washed with 15 mL of Et_2O 3 times. The solid was redissolved in MeOH, filtered, and the solvent was removed under reduced pressure to yield 136 mg (68.3%) of product.

Synthesis of [Ru(tpy)(pyalk)(Cl)]Cl·3H_2O·MeCN ([1]Cl)

$Ru(tpy)Cl_3$ (299 mg, 678 µmol) and pyalkH (105 mg, 764 µmol, 1.13 equiv) were placed under nitrogen atmosphere. A nitrogen sparged solution of N-ethylmorpholine (86 µL, 78 mg, 680 µmol, 1 equiv) in 36 mL of 5:1 ethanol:water was added to the reaction mixture. The reaction mixture was then heated to 97°C for 4 hours, over which time the reaction mixture turned a dark purple color. The solution was then removed from heat, allowed to cool to room temperature, and filtered through Celite 545. The precipitate was washed with water, and the solvent was removed from the combined filtrates under vacuum. The isolated black solid was redissolved in a small amount of water and purified via reverse-phase flash chromatography using a mixture of acetonitrile and water as the mobile phase and a 15.5g RediSep C18 GOLD column as the stationary phase. Solvent was removed under vacuum from the product-containing dark purple fractions, which was then dried in a vacuum desiccator yielding 113 mg (31%) of product as a hygroscopic black powder. Calculated: C 47.17, H 4.75, N 11.00; Found: C 47.10, H 5.20, N 11.30.

Crystallization of [Ru(tpy)(pyalk)Cl]BPh_4 ([1]BPh_4)

A solution of saturated $NaBPh_4$ was added dropwise to a solution of **[1]Cl** (20 mg) in water, resulting in immediate formation of a dark grey precipitate. Additional $NaBPh_4$ solution was added until no more precipitate formed. This precipitate was washed with water and dissolved in dichloromethane (DCM). The DCM solution was then dried with anhydrous $MgSO_4$ and filtered. Vapor diffusion of diethyl ether into this solution yielded the solvento-complex, **[1]$BPh_4 \cdot 2CH_2Cl_2$**, as dark red crystals suitable for X-ray diffraction studies.

Crystal structure determination

Crystals were mounted on MiTeGen's MicroLoops using Immersion oil, type NVH by Cargille and cooled to 110 K in a stream of cold N_2 gas. Diffraction data were collected using a Bruker APEX2 Duo CCD area detector diffractometer with the detector positioned at a distance of 4.0 cm from the crystal. The X-ray source was sealed tube Mo-Kα radiation (λ= 0.71073 Å). Data were processed (integrations and multi-scan absorption corrections) by Bruker-AXS software Apex3 v2017.3-0. Using Olex2 software,[29] the structures were solved by Intrinsic Phasing using ShelXT[30] and refined anisotropically on F2 with ShelXL.[31] All hydrogen atoms were refined isotopically.

Procedure for Electrochemical Measurements

Electrochemical measurements were obtained using a Pine WaveDriver potentiostat with platinum working (1.6 mm OD) and counter electrodes. For aqueous measurements an Ag/AgCl electrode in a saturated KCl solution was used as the reference electrode. For measurements in non-aqueous solvents, an Ag/Ag^+ electrode the same electrolyte solution used for measurements was used as a pseudo-reference electrode. Absolute potentials were obtained by referencing to Fc/Fc^+ as both an external and internal standard.[32,33] All measurements were compared with the specified electrolyte solution as a blank measurement under identical electrode conditions.

Procedure for UV-Visible Measurements

This journal is © The Royal Society of Chemistry 20xx

UV-visible measurements were collected on a PerkinElmer Lambda 465 spectrophotometer. Solutions for UV-visible measurements were prepared by dissolving solid **[1]Cl** in solvent using volumetric glassware to obtain the indicated concentrations. Standard measurements were taken using a quartz cuvette with a 1 cm path length. Spectroelectrochemical spectra were taken using an optical thin layer (OTL) cell and a Pine gold honeycomb electrode with an effective path length of 1.7 mm. Prior to measuring the UV-visible spectra, a rapid CV was taken using the honeycomb electrode to confirm no change in electrochemical behavior occurred due to the use of the honeycomb electrode. A constant potential was then applied, and UV-visible spectra were recorded once a constant current was obtained, generally within 10 seconds.

Procedure for C-H Bond Oxidant Screening

A 1.00 mg/mL stock solution of **[1]Cl** (3.0 mL, 3.0 mg, 4.7 µmol), 3-(trimethylsilyl)propionic-2,2,3,3-d_4 acid sodium salt (3.3 mg, 19 µmol), and 2.4 mmol of the chemical oxidant were dissolved in 7.0 mL of D_2O. The reaction flask was then stoppered, THF (40 µL, 624 µmol) was added, and the reaction solution stirred for 1 hour at room temperature (20° C). A ^1H NMR of the solution was then collected. For reactions under N_2 atmosphere, the solid reactants were placed under vacuum using standard Schlenk techniques, and the D_2O was sparged for a minimum of 30 minutes. For reactions undertaken with exclusion of light, the reaction flask was wrapped in aluminum foil prior to addition of the THF.

Procedure for C-H Bond Substrate Scope Screening

CAN (100 mg, 183 µmol) was dissolved in 150 µL acetonitrile and 250 µL of a 13.5 mM stock solution of **2** prepared by dissolving **[1]Cl** in water. To this solution 12 µL (~100 µmol) of substrate were added, and the reaction was stirred for the specified duration(s). The reaction was then quenched with 100 mg (793 µmol) sodium sulfite, and filtered through glass wool. The reaction vessel was washed with 2 mL of ethyl acetate and 2 mL of water, which was added to the filtered reaction solution. Acetophenone (10 µL, 97 µmol was added to the filtered reaction solution as an internal standard, and the aqueous fraction was extracted ethyl acetate (2 x 2 mL). The combined organic fractions were then extracted with 5 mL of brine to remove any remaining **2** and CAN, dried with $MgSO_4$, filtered, and analyzed via GC.

Procedure for GC Measurements

Product yields determined by GC were obtained using a Thermo Scientific Trace 1300 GC with a flame ionization detector (FID), and a TG-1301MS column. Substrate scope screening results were analyzed by injecting 10 µL of the processed samples onto the column using a split/splitless injection port in a 1:5 split ratio. Concentration-response curves were obtained for each of the products analyzed by injecting 10 µL of a known concentration of each of the identified products using the same GC settings above. The FID response was measured at a minimum of 5 separate concentrations for each product, and the FID response for each concentration was measured 3 times. The effect of the purification process on product yield was determined by measuring the FID response for product samples of known concentration after following the same purification procedure used for the substrate scope screening.

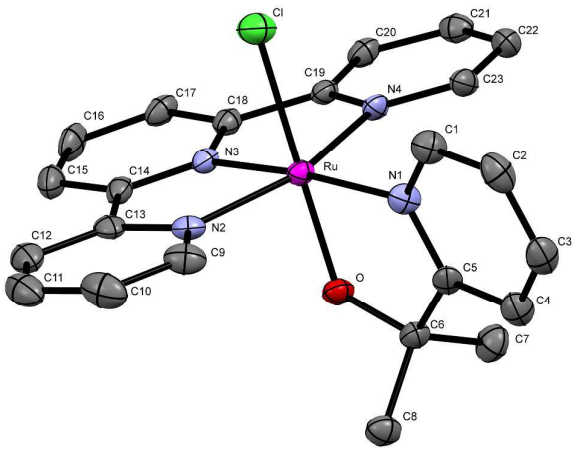

Fig. 1 Thermal ellipsoid plot of the molecular unit of **[1]BPh_4·$2CH_2Cl_2$** showing 50% probability ellipsoids; hydrogen atoms, counteranions, and lattice solvent molecules omitted for clarity. Color coding: grey, C; blue, N; red, O; green, Cl; magenta, Ru.

Results

Structural Properties of $[Ru(tpy)(pyalk)Cl]^+$ (1)

Structural parameters for **[1]BPh_4** were determined by X-ray diffraction after exchanging the outer-sphere chloride anion for a tetraphenyl borate anion to promote crystal growth (Fig. 1). As visible in the crystal structure, the O-atom of the pyalk ligand binds trans to the inner sphere Cl ligand, as expected from a comparison of the relative kinetic trans effects of the ligand moieties (RO^-<py<Cl^-).[34] The Ru-Cl bond length of 2.383 Å is somewhat shorter than that seen in $[Ru(tpy)(phpy)Cl]PF_6$ (2.443 Å),[35] consistent with a weaker trans influence by the alkoxide moiety in **1** relative to the phenyl group in $[Ru(tpy)(phpy)Cl]^+$. Both the Ru-Cl and Ru-O (1.921 Å) bond lengths in **1** are very similar to the Ru-Cl (2.336 and 2.405 Å) and Ru-O (1.929 and 1.949 Å) bond lengths found in the related Ru(III/III) dimer $\{[RuCl(tpy)]_2(\mu\text{-Hpbl-}\kappa\text{-}N_2O_2)\}(PF_6)_2\cdot MeOH$,[25] supporting the assignment of **1** as a Ru(III) complex containing an anionic alkoxide ligand. Full crystallographic data has been deposited with the CCDC (#1838681).

Redox Properties of $[Ru(tpy)(pyalk)Cl]^+$ (1)

The redox properties of **1** were determined via cyclic voltammetry (CV) (Fig. 2) by dissolving **[1]Cl** in acetonitrile. Three quasi-reversible redox waves are apparent in the CV, the first at 0.07 V vs. NHE, the second at 1.224 V vs. NHE, and the third at 1.60 V vs. NHE. The wave at 1.224 V vs. NHE was identified as chloride oxidization at the electrode by collecting a CV of tetramethylammonium chloride under identical conditions (Fig. S1).

In order to assign these redox waves, the UV-visible spectra of **[1]Cl** was recorded at applied potentials above and below

each of the waves (Fig. 4). As shown, applying a voltage below 0.07 V vs. NHE results in a dramatic red-shift of the d-π*(tpy) MLCT band from 446 nm to 584 nm, as well as the appearance of a second absorption band at ~476 nm, possibly a d-π*(pyalk) MLCT.[24,28] In addition to these well-defined peaks, a broad absorbance is also observed between ca. 650 and 950 nm upon reduction. Broad absorption of this nature has sometimes been observed in Ru(II) complexes,[28] and have been previously assigned as d-dπ and dπ-π* transitions between mixed ligand-metal orbitals.[36] Application of potentials between 0.07 and 1.224 V vs. NHE results in regeneration of the original spectra. Applying potentials > 1.6 V vs. NHE results in a blue-shift of the MLCT to ~430 nm (Fig. 3). As expected for oxidation of Cl^-, no significant change is observed upon application of potentials between 1.224 and 1.6 V vs. NHE. Based on these results, the wave at 0.07 V can be assigned as the Ru(II/III) redox couple, and the wave at 1.6 V vs. NHE can be assigned as the Ru(III/IV) redox couple.

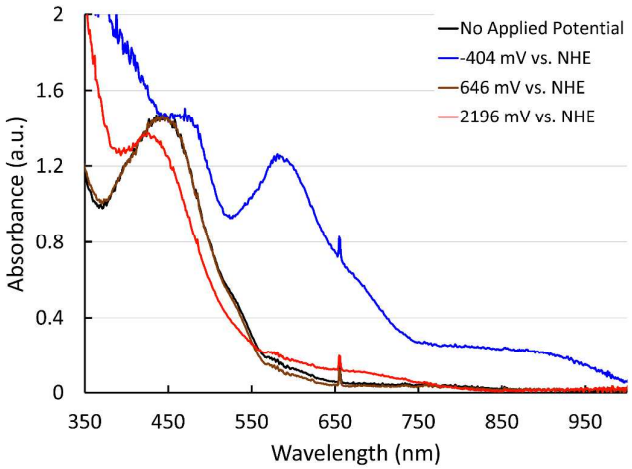

Fig. 3 UV-visible spectra of 2.5 mM **[1]Cl** in acetonitrile containing 100 mM $[Bu_4N][PF_6]$ as an electrolyte with constant application of the potentials indicated.

Redox Properties of $[Ru(tpy)(pyalk)(OH)]^+$ (2) and $[Ru(tpy)(phpy)(H_2O)]^{2+}$ (3)

Relative to its behavior in acetonitrile, in phosphate buffer **1[Cl]** shows much simpler redox chemistry, with only one reversible wave observed (Fig. 4). The potential of this redox event is pH dependent, showing the characteristic 59 mV/pH unit shift of a one proton per electron proton-coupled electron transfer (PCET) below pH ~7.5, and having a constant value of 0.124 V vs. NHE above that pH (Fig. 5). This pH dependent behavior indicates the presence of a labile proton with a pK_a of approximately 7.5. This pK_a is significantly more alkaline than expected for the bound pyalk ligand, and somewhat more acidic than the related $[Ru(tpy)(Hpbl)(H_2O)]^+$ complex.[24] This pH dependence suggests rapid exchange of the chloride ligand for solvent upon dissolution of **1[Cl]** to form $[Ru(tpy)(pyalk)(OH)]^+$, **2**. This solvation in aqueous solution is supported by the d-π*(tpy) MLCT observed in the UV-visible spectrum of **1[Cl]** in water (Fig. 6), which is blue-shifted relative to that observed for **1[Cl]** in acetonitrile. Upon application of potentials more reducing that this wave, a distinct red-shift from 450 to 475 nm is observed for the d-π*(tpy) MLCT. Based on this data we can confidently assign this redox event as a Ru(II/III) couple.

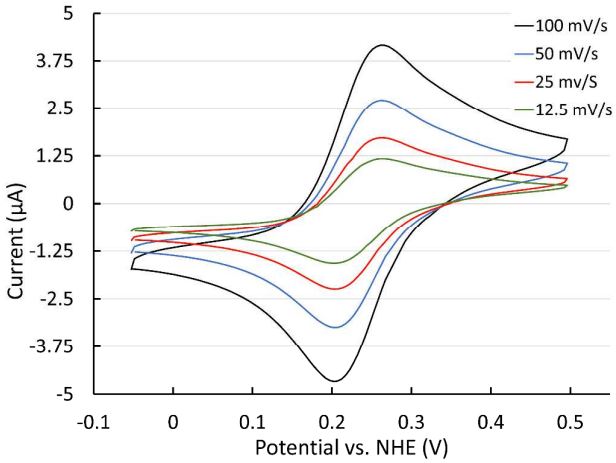

Fig. 4 Cyclic voltammograms of 1.57 mM **1[Cl]** in 100 mM pH 6.86 aqueous P_i buffer at the indicated potential sweep rates. Referenced to saturated Ag/AgCl and converted to NHE using the standard value Ag/AgCl = 197 mV vs. NHE.[33]

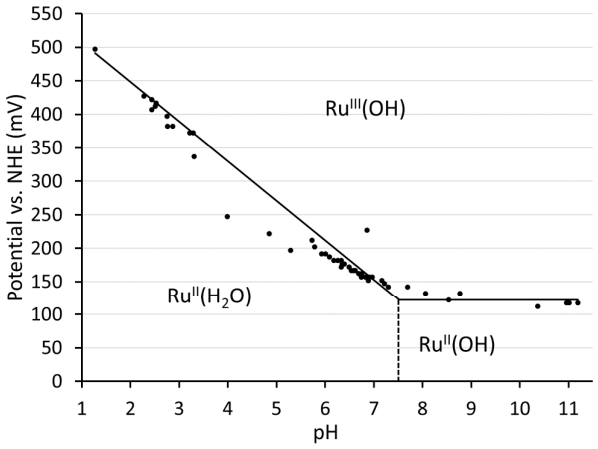

Fig. 5 Pourbaix diagram of 1.3 mM **2** in 100 mM aqueous P_i buffer. Referenced to saturated Ag/AgCl and converted to NHE using the standard value Ag/AgCl = 197 mV vs. NHE.[33]

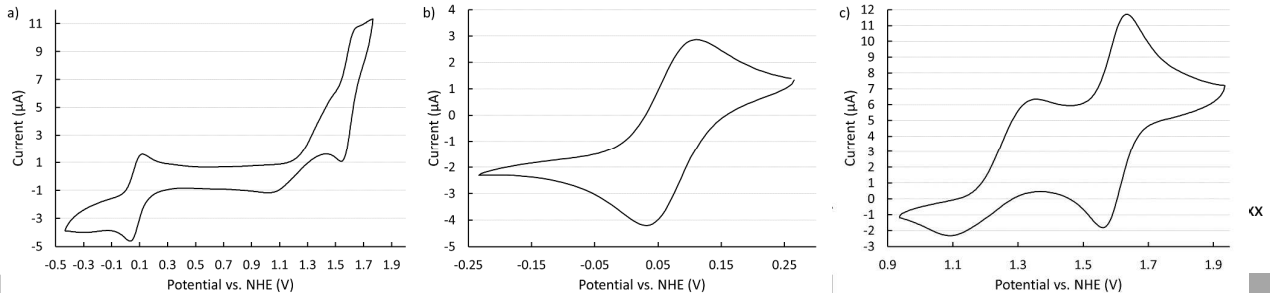

Fig. 2 Cyclic Voltammograms of 2.5 mM **[1]Cl** 100 mV/s (a) and 50 mV/s (b,c) in acetonitrile containing 100 mM $[Bu_4N][PF_6]$ as electrolyte. Potentials referenced to Fc/Fc^+ and converted to NHE using the standard values Fc/Fc^+ = 400 mV vs SCE[32] and SCE = 241 V vs. NHE.[33]

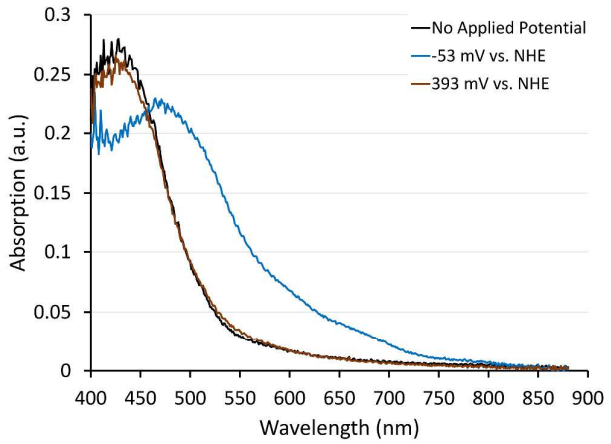

Fig. 6 UV-visible spectra of 500 µM **[1]Cl** in 100 mM aqueous P_i buffer with constant application of the potentials indicated.

In order to compare the effects of the pyalk ligand on the pH dependent redox behavior of **2** to other Ru complexes ligated to tpy and an anionic ligand, we generated a Pourbaix diagram for [Ru(tpy)(phpy)Cl] (Fig. 7, phpy = 2-phenylpyridine). Based on the observed pH dependence of the Ru(II/III) couple and comparison to the related complex $Ru(dpp)(bpy)(H_2O)]^{2+}$ (dpp = 1,3-di(pyrid-2-yl)benzene),[37] upon dissolution in P_i buffer [Ru(tpy)(phpy)Cl] forms a solvento complex similar to that formed by **2**, i.e. $[Ru(tpy)(phpy)(H_2O)]^+$, **3**. At higher pH values, **3** appears to undergo anation by the P_i buffer, the details of this reaction are currently under investigation.

While both **2** and **3** show similar Ru(II/III) potentials at pH 1, the pH dependence of these potentials differs substantially due to differences in the pK_a values for the complexes. Specifically, the differences in pK_a values cause the Ru(II/III) potential of **3** to remain constant at ~410 mV vs. NHE between pH 1 and ~6.5, while that of **2** decreases dramatically over this pH region. This results in **2** having a lower Ru(II/III) potential than **3** at pH values above ~2.8.

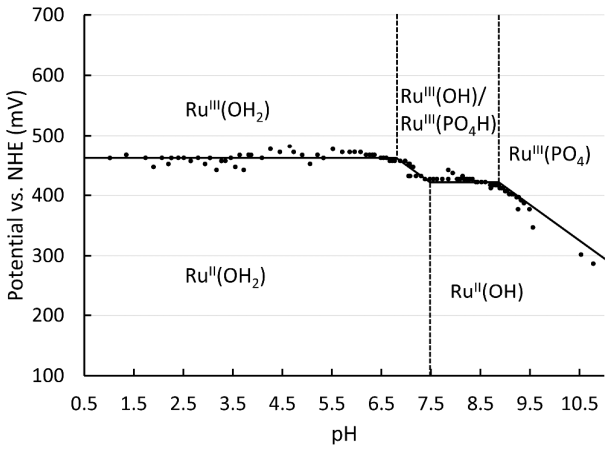

Fig. 7 Pourbaix diagram for 1.7 mM **3** in 100 mM aqueous P_i buffer. Referenced to saturated Ag/AgCl and converted to NHE using the standard value Ag/AgCl = 197 mV vs. NHE.[33]

C-H Bond Oxidation Activity of $[Ru(tpy)(pyalk)(OH)]^+$ (2)

The ability of **1[Cl]** to catalyze C-H bond oxidation was screened via ^1H NMR with a variety of oxidants using THF as a substrate (Table 1). Of the oxidants screened, only cerium(IV) ammonium nitrate (CAN) yielded any THF oxidation products. Following this initial screen, we studied the effect of air and light on the oxidation of THF by CAN catalyzed by **1[Cl]**, finding no measurable effect based on either of these factors (Table S1). Based on these results, we examined the substrate scope of C-H bond oxidation by **1[Cl]** with CAN via initial identification of products via GC-MS followed by quantitation using GC. As shown in Table 2, **1[Cl]** is capable of catalysing both alkene epoxidation and aliphatic C-H bond hydroxylation. Conversion for these reactions is rather modest, although alkene epoxidation shows significantly greater product yields than alkane oxidation to ketones.

Table 1 Overall conversion and oxidized product yields for THF oxidation by **1[Cl]** using various chemical oxidants.[a]

Oxidant	Yield[b] γ-Butyrolactone	Yield[b] Succinic Acid	Remaining Starting Material[c]
H_2O_2	0%	0%	87%
$NaIO_4$	0%	0%	96%
CAN	25.8%	3.7%	59%
CAN[*]	0%	0%	98%

[a]Reaction conditions: 4.7 µmol **1** (0.95% catalyst loading), 2.4 mmol oxidant, 493 µmol THF in 10 mL D_2O containing 19 µmol 3-(trimethylsilyl)propionic-2,2,3,3-d_4 acid sodium salt as an internal standard at 20° C under air for 1 hr. [b]As determined by ^1H NMR, mol product/initial mol THF. [c]As determined by ^1H NMR, mol THF/initial mol THF. [*]No catalyst added.

Table 2 Overall conversion and GC product yields for substrate oxidation by **1** using CAN.[a]

Substrate	Major Product (% yield[b])	Remaining Starting Material (%[b])
Cyclooctane	Cyclooctanone (3.8 ± 0.4)	48.9 ± 0.4
Ethylbenzene[c]	Acetophenone (5.4 ± 1.1)	32.6 ± 5.2
Cyclooctene	Cyclooctene Oxide (30.2 ± 0.3)	23.2 ± 1.1

[a]Reaction conditions: 3.1 µmol **1** (~4.1% catalyst loading), 390 µmol CAN, 10 µL substrate (~75 µmol) in 400 µL 1:2 MeCN:H_2O under air for 1 hr. [b]Average of a minimum of 3 runs, error represents 1 standard deviation from the mean, mol product/initial mol starting material. [c]Reaction time of 2 hrs.

Discussion

Redox Properties of $[Ru(tpy)(pyalk)Cl]^+$ (1), $[Ru(tpy)(pyalk)(OH)]^+$ (2), and $[Ru(tpy)(phpy)(H_2O)]^{2+}$ (3)

Our goal in synthesizing **1[Cl]** was to lower the potentials of the Ru(II/III) and Ru(III/IV) redox couples. We therefore began our analysis by characterizing **1** electrochemically. In acetonitrile, **1** is observed to have Ru(II/III) and Ru(III/IV) redox potentials of 0.07 and 1.60 V vs. NHE, respectively. This Ru(II/III) redox couple is at a significantly lower potential than the related complexes [Ru(tpy)(phpy)Cl] and [Ru(tpy)(bhq)Cl] (Table 3), as well as the dimeric complex $\{[RuCl(tpy)]_2(\mu\text{-Hpbl-}\kappa\text{-}N_2O_2)\}$, which has a Ru(II,II/III,III) redox potential of 0.54 V vs.

NHE and has the same inner-sphere coordination environment.[25] This extremely low Ru(II/III) redox potential clearly indicates that **1** has two anionic ligands in the coordination sphere in acetonitrile solution. Therefore: a) **1** retains its chloride ligand in MeCN and b) the pyalk ligand is deprotonated.

While inclusion of the strong-donor pyalk ligand successfully lowered the Ru(II/III) couple relative to other ligand sets, very little change was seen in the Ru(III/IV) potential. Indeed **1** has potentials quite similar to those of $[Ru(bpy)_2Cl_2]$, which has Ru(II/III) and Ru(III/IV) couples at 0.0 and 1.7 V vs. NHE, respectively.[15] This large difference in the Ru(II/III) and Ru(III/IV) couples is typical of Ru complexes that cannot undergo PCET, as charge buildup on the complex inhibits further oxidation. One simple method to enable PCET for Ru chloride complexes is to dissolve them in water, which commonly results in the formation of an aqua complex capable of deprotonation via hydrolysis.[15]

Table 3 Ru(II/III) couples in aprotic solvent for complexes bearing two anionic ligands.

Complex[a]	Ru(II/III) Potential (V vs. NHE)[b]	Reference
1	0.07[c]	[d]
[Ru(tpy)(phpy)Cl]	0.46[c]	[35]
[Ru(tpy)(bhq)Cl]	0.48[e]	[28]
cis,cis-$[RuCl_2(Hbpp)(DMSO)_2]$	1.081[c]	[38]
$[Ru(bpy)_2Cl_2]$	0.0[c]	[15]

[a]Ligand abbreviations used: bhq = benzo[h]quinoline, Hbpp = 3,5-bis(2-pyridyl)pyrazole. [b]Converted to NHE using the standard value SSCE = 241 mV vs. NHE.[33] [c]Measured in MeCN. [d]This work. [e]Measured in DMF.

Indeed, upon dissolution in water the inner sphere chloride of **[1]Cl** exchanges with solvent to form the Ru(III) hydroxide complex **2** (Scheme 2). Unlike **1**, the Ru(II/III) redox couple in **2** is clearly proton-coupled below pH ~7.5, as shown in its Pourbaix diagram (Fig. 6). Despite this success in enabling PCET at the Ru center in **2**, no Ru(III/IV) couple is observed for **2** within the solvent window of the phosphate buffer. This indicates that while oxidation of **2** to form the type of Ru(IV) oxo species typically involved in C-H bond oxidation may be possible, it will require oxidants with one-electron redox potentials above 1.23 V vs. RHE (reversible hydrogen electrode).

$$\underset{\textbf{[1]Cl}}{[Ru(tpy)(pyalk)Cl]Cl} \xrightarrow[H_2O]{} \underset{\textbf{2}}{[Ru(tpy)(pyalk)(OH)]^+} + H_3O^+ + Cl^-$$

Scheme 2. Formation of **2** upon dissolution of **[1]Cl** in water.

Comparison between **2** and other Ru complexes bearing tpy and other anionic ligands such as phpy (Fig. 8 and Table 4) shows little difference in the Ru(II/III) potentials at pH 1. Comparison of proton-coupled redox potentials at a single pH value can be misleading however, as differences in pK_a values can cause dramatic differences in their pH dependence. In order to address this concern, we searched for a Pourbaix diagram of the related organometallic complex **3**, where the alkoxide group has been replaced with a carbanion. Despite the well-characterized redox properties of [Ru(tpy)(phpy)Cl] in MeCN,[35] and DMF,[17,28] the most closely related complex we could find data for in aqueous solution was $[Ru(dpp)(bpy)(H_2O)]^{2+}$.[40] We were unable to locate any studies where **3** was used in aqueous solution, and are therefore including its Pourbaix diagram in this manuscript (Fig. 7).

Table 4 Ru(II/III) redox potentials in pH 1 aqueous solution for selected complexes bearing anionic ligands.

Complex[a]	Ru(II/III) Potential (V vs. NHE)[b]	Reference
2	0.50	[c]
$[Ru(tpy)(phpy)(H_2O)]^{2+}$	0.46	[c]
$[Ru(tpy)(Hpbl)(H_2O)]^{2+}$	0.48	[24]
trans-$[Ru(tpy)(pic)(H_2O)]^{2+}$	0.73	[39]
cis-$[Ru(tpy)(pic)(H_2O)]^{2+}$	0.83	[39]
$[Ru(dpp)(bpy)(H_2O)]^{2+}$	0.30	[40]
$[Ru(bda)(isoqF)_2]^+$	0.70	[40]
$[Ru(bda)(ptzBr)_2]^+$	0.60	[40]

[a]Ligand abbreviations used: phpy = 2-phenylpyridine, Hpbl = 3,5-bis(2-pyridyl)pyrazole, pic = 2-picolinic acid, dpp = 1,3-di(pyrid-2-yl)benzene, bda = 2,2'-bipyridine-6,6'-dicarboxylic acid, isoqF = 6-fluoroisoquinoline, ptzBr = 6-bromophthalazine. [b]At pH 1, potentials converted to NHE using the standard value SCE = 241 mV vs. NHE and Ag/AgCl = 197 mV vs. NHE.[33] [c]This work.

Comparison of the Pourbaix diagrams of **2**, **3**, and $[Ru(dpp)(bpy)(H_2O)]^{2+}$ reveals that both **3** and $[Ru(dpp)(bpy)(H_2O)]^{2+}$ have very similar behavior in water, as expected from two complexes bearing 4 N and 1 C donor ligands. The primary difference in the two complexes is the higher pK_a observed for **3** (~6.5 vs ~4.9 for $[Ru(dpp)(bpy)(H_2O)]^{2+}$).[40] In contrast, the aqua ligand on **2** is significantly more acidic than those in **3** and $[Ru(dpp)(bpy)(H_2O)]^{2+}$ in both the Ru(II) (pK_a ~7.5) and Ru(III) (pK_a < 1) oxidation states. This dramatic shift occurs despite the fact that the O-donor pyalk ligand is expected to provide more e^- density to the Ru center relative to the organometallic dpp and phpy ligands based on its inability to serve as a π-acceptor and the relative potentials of **2** and **3** in MeCN (Table 3). The precise reasons for this pK_a shift are currently under investigation, but may be due to the ability of the pyalk ligand to form H-bonds to water in aqueous solution. This competition between the pK_a values and the non-proton coupled Ru(II/III) potentials is responsible for the fact that both **2** and **3** have similar Ru(II/III) potentials under acidic conditions. In contrast, under neutral to alkaline conditions, the Ru(II/III) couple of **2** is significantly lower than that seen for **3**.

C-H Bond Oxidation Activity of $[Ru(tpy)(pyalk)(OH)]^+$ (2)

In order to test the ability of **2** to catalyze C-H bond oxidation, we monitored the oxidation of the model substrate THF with various oxidizing agents (Table 1). Only CAN was found to be capable of driving oxidation catalysis by **2**. Based on the redox potentials observed for **1** and **2**, this is most likely due to the need for a one-electron oxidation of Ru(III) to Ru(IV) in the catalytic cycle, i.e. none of the two-electron oxidants

This journal is © The Royal Society of Chemistry 20xx

employed are expected to be thermodynamically capable of oxidizing **2** from Ru(III) to Ru(V).

Two distinct reactions are catalyzed by **2** in water, the oxidation of aliphatic C-H bonds to ketones, as exemplified by THF oxidation to γ-butyrolactone, and alkene epoxidation, as exemplified by the conversion of cyclooctene to cyclooctene oxide. Unfortunately, both of these reactions proceed with only modest turnover, and a significant number of overoxidation products are observed. This is likely due to a similar pathway as observed for $[Ru(bpy)_2(py)O]^{2+}$,[41] where two-electron Ru(II/IV) reactions compete with one-electron Ru(III/IV) reactions.

Conclusions

While we initially hypothesized that the pyalk ligand would reduce the overall potential necessary to form Ru(IV)=O species needed to catalyze C-H bond oxidation, only the Ru(II/III) potential of **1** and **2** was greatly affected by using this ligand, and the potential needed to form a Ru(IV)=O was not lowered significantly in either water or acetonitrile solvents. Indeed, the overall Ru(III/IV) potential of **1** in acetonitrile was found to be almost identical to that of $Ru(bpy)_2Cl_2$, despite the inclusion of the O-donor pyalk ligand. In acetonitrile this is likely due to the inability of **1** to participate in PCET due to the quite low pK_a of the bound pyalk ligand. The overall Ru(II/III) potential of **2** in aqueous solution at pH 1 is comparable to that of the organometallic complex **3**, but this is primarily due to the much lower pK_a values of **2** in both the Ru(II) and Ru(III) oxidation states. Above pH 3, **2** has a lower Ru(II/III) potential than **3**.

Despite its relatively low Ru(II/III) potential, **2** was found to only catalyze C-H bond oxidation using the one-electron oxidant CAN due to the large potential difference between the Ru(II/III) and Ru(III/IV) redox potentials. This need to use CAN to drive catalysis limits the usefulness of **2** relative to other Ru-based C-H bond oxidation catalysts that have been reported,[1–3] as it leads to overoxidation and very low atom economy. In order to overcome this limitation, we are currently investigating strategies for fostering two-electron chemistry at Ru by lowering the Ru(III/IV) potential, e.g. PCET.[15,42]

Conflicts of interest

The authors have no conflicts of interest to declare.

Acknowledgements

The authors would like to thank North Dakota State University, the NDSU College of Science and Math, the NDSU Office of the Provost, and the NDSU Department of Chemistry and Biochemistry for funding support. This work was further supported by the NSF EPSCoR Innovative and Strategic Program Initiatives for Research and Education-North Dakota (INSPIRE-ND) Award #IIA-1355466 for funding. ARP would like to thank Profs. Mukund Sibi (NDSU), Pinjing Zhou (NDSU), and Jayaraman Sivaguru (BGSU) for their support and suggestions.

Notes and references

1 A. E. Shilov and G. B. Shul'pin, *Chem. Rev.*, 1997, **97**, 2879–2932.
2 R. H. Crabtree, *J. Chem. Soc. Dalton Trans.*, 2001, **0**, 2437–2450.
3 M. C. White, *Science*, 2012, **335**, 807–809.
4 M. Costas, *Coord. Chem. Rev.*, 2011, **255**, 2912–2932.
5 T. Nanjo, E. C. de Lucca and M. C. White, *J. Am. Chem. Soc.*, 2017, **139**, 14586.
6 B. G. Hashiguchi, S. M. Bischof, M. M. Konnick and R. A. Periana, *Acc. Chem. Res.*, 2012, **45**, 885–898.
7 G. Song, F. Wang and X. Li, *Chem. Soc. Rev.*, 2012, **41**, 3651–3678.
8 J. F. Hartwig, *J. Am. Chem. Soc.*, 2016, **138**, 2–24.
9 W. Nam, *Acc. Chem. Res.*, 2007, **40**, 522–531.
10 B. Li and P. H. Dixneuf, *Chem. Soc. Rev.*, 2013, **42**, 5744–5767.
11 G. Olivo, M. Nardi, D. Vìdal, A. Barbieri, A. Lapi, L. Gómez, O. Lanzalunga, M. Costas and S. Di Stefano, *Inorg. Chem.*, 2015, **54**, 10141–10152.
12 Y. Kawamata, M. Yan, Z. Liu, D.-H. Bao, J. Chen, J. T. Starr and P. S. Baran, *J. Am. Chem. Soc.*, 2017, **139**, 7448–7451.
13 M. Zhou and R. H. Crabtree, *Chem. Soc. Rev.*, 2011, **40**, 1875–1884.
14 Z. Chen and G. Yin, *Chem. Soc. Rev.*, 2015, **44**, 1083–1100.
15 T. J. Meyer and M. H. V. Huynh, *Inorg. Chem.*, 2003, **42**, 8140–8160.
16 S.-I. Murahashi and D. Zhang, *Chem. Soc. Rev.*, 2008, **37**, 1490–1501.
17 S. Aiki, Y. Kijima, J. Kuwabara, A. Taketoshi, T. Koizumi, S. Akine and T. Kanbara, *ACS Catal.*, 2013, **3**, 812–816.
18 T. Hirano, K. Ueda, M. Mukaida, H. Nagao and T. Oi, *J. Chem. Soc. Dalton Trans.*, 2001, **0**, 2341–2345.
19 D. H. Gibson, J. G. Andino and M. S. Mashuta, *Organometallics*, 2005, **24**, 5067–5075.
20 O. Johansson and R. Lomoth, *Chem. Commun.*, 2005, **0**, 1578–1580.
21 H. Nagao, K. Enomoto, Y. Wakabayashi, G. Komiya, T. Hirano and T. Oi, *Inorg. Chem.*, 2007, **46**, 1431–1439.
22 Taher Deeb, Thibault Michelle E., Di Mondo Domenico, Jennings Michael and Schlaf Marcel, *Chem. – Eur. J.*, 2009, **15**, 10132–10143.
23 H. Giglmeier, T. Kerscher, P. Klüfers, D. Schaniel and T. Woike, *Dalton Trans.*, 2009, **0**, 9113–9116.
24 L. Francàs, R. M. González-Gil, A. Poater, X. Fontrodona, J. García-Antón, X. Sala, L. Escriche and A. Llobet, *Inorg. Chem.*, 2014, **53**, 8025–8035.
25 L. Francàs, R. M. González-Gil, D. Moyano, J. Benet-Buchholz, J. García-Antón, L. Escriche, A. Llobet and X. Sala, *Inorg. Chem.*, 2014, **53**, 10394–10402.
26 Y.-L. Wong, Q. Yang, Z.-Y. Zhou, H. K. Lee, T. C. W. Mak and D. K. P. Ng, *New J. Chem.*, 2001, **25**, 353–357.
27 B. P. Sullivan, J. M. Calvert and T. J. Meyer, *Inorg. Chem.*, 1980, **19**, 1404–1407.
28 P. G. Bomben, K. C. D. Robson, P. A. Sedach and C. P. Berlinguette, *Inorg. Chem.*, 2009, **48**, 9631–9643.
29 O. V. Dolomanov, L. J. Bourhis, R. J. Gildea, J. a. K. Howard and H. Puschmann, *J. Appl. Crystallogr.*, 2009, **42**, 339–341.
30 G. M. Sheldrick, *Acta Crystallogr. Sect. Found. Adv.*, 2015, **71**, 3–8.

31 G. M. Sheldrick, *Acta Crystallogr. A*, 2008, **64**, 112–122.
32 N. G. Connelly and W. E. Geiger, *Chem. Rev.*, 1996, **96**, 877–910.
33 A. J. Bard and L. R. Faulkner, *Electrochemical Methods: Fundamentals and Applications*, Wiley, New York, 2nd ed., 2000.
34 B. J. Coe and S. J. Glenwright, *Coord. Chem. Rev.*, 2000, **203**, 5–80.
35 H. Hadadzadeh, M. C. DeRosa, G. P. A. Yap, A. R. Rezvani and R. J. Crutchley, *Inorg. Chem.*, 2002, **41**, 6521–6526.
36 E. J. Viere, A. E. Kuhn, M. H. Roeder, N. A. Piro, W. S. Kassel, T. J. Dudley and J. J. Paul, *Dalton Trans.*, 2018, **47**, 4149–4161.
37 T. Wada, T. Hiraide and Y. Miyazato, *ChemistrySelect*, 2016, **1**, 3045–3048.
38 C. Sens, M. Rodríguez, I. Romero, A. Llobet, T. Parella, B. P. Sullivan and J. Benet-Buchholz, *Inorg. Chem.*, 2003, **42**, 2040–2048.
39 A. Llobet, P. Doppelt and T. J. Meyer, *Inorg. Chem.*, 1988, **27**, 514–520.
40 L. Wang, L. Duan, Y. Wang, M. S. G. Ahlquist and L. Sun, *Chem. Commun.*, 2014, **50**, 12947–12950.
41 L. K. Stultz, R. A. Binstead, M. S. Reynolds and T. J. Meyer, *J. Am. Chem. Soc.*, 1995, **117**, 2520–2532.
42 D. R. Weinberg, C. J. Gagliardi, J. F. Hull, C. F. Murphy, C. A. Kent, B. C. Westlake, A. Paul, D. H. Ess, D. G. McCafferty and T. J. Meyer, *Chem. Rev.*, 2012, **112**, 4016–4093.

This journal is © The Royal Society of Chemistry 20xx

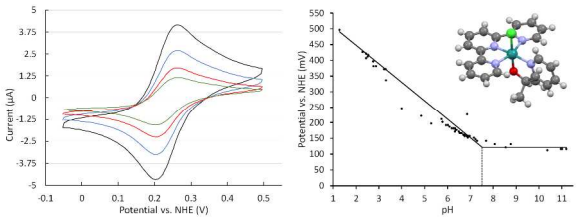

An O-donor ligand leads to low Ru(II/III) potentials.